Crack Development in Concrete due to Moisture Flow

D. Jankovic
Delft University of Technology
Faculty of Civil Engineering and GeoSciences
Microlab

J.G.M. van Mier
ETH Hönggerberg, CH-8093 Zürich
Switzerland
Formerly at Microlab, TU Delft

The goal of this study is to develop a numerical model for the simulation of crack growth due to moisture flow in the porous zone between aggregate and matrix (interfacial transition zone, ITZ), where cracking in concrete originates. Two models are coupled based on similarities in their mesh shape: a Lattice Gas Automaton for moisture flow and a Lattice Fracture Model for crack growth. The results of coupling analyses are presented for several cases.

Key words: **Moisture Flow, Lattice Gas Automaton, Lattice Fracture Model, Interfacial Transition Zone, Concrete**

1 Introduction

Research on concrete has traditionally focused on the mechanical properties, more specifically on fracture. Two criteria are considered for the analysis of failure of the material: a strength and a fracture energy criterion. According to the strength criterion, concrete fails when tensile stresses, induced by the mechanical load, exceed material tensile strength while in the fracture energy criterion, in order for a crack to grow, a certain amount of energy is required.
Rarely any research gives attention to the origin of the cracks in concrete. This study focuses on the cause of cracking in particular in the zone between aggregate and cement matrix (interfacial transition zone). Although no mechanical load is applied, cracks may initiate here due to significant volume changes and develop to cause complete material failure. New observations (Martinola & Wittmann 1995, Sadouki & Van Mier 1997) showed that moisture flow and the associated drying might cause shrinkage strains and stresses large enough for concrete to crack. Shrinkage induces deformations and hence volume changes which may lead to internal stresses in concrete. When high stress concentrations appear in or close to the ITZ, early cracking may occur. Three physical mechanisms might be the cause of internal stresses in the concrete ITZ: thermal gradients (due to the exothermic hydration reactions in cement), chemical (or autogeneous) shrinkage and swelling or shrinkage caused by moisture movements. Here we bring into focus the drying shrinkage only

and the effect on eigen-stresses and crack growth in the ITZ.

The phenomenon of shrinkage in cement paste itself is not yet fully understood (Xi & Jennings 1992). Drying shrinkage of the cement paste is just one of the types of shrinkage that might occur while moisture flow is present. Due to the volume change eigen-stresses may build up and eventually cause microcracks. Under subsequent mechanical load, all kinds of durability problems might develop. The numerous mechanisms that cause drying shrinkage (Xi & Jennings 1992) are visible only at the micro-level. Thus it is necessary to go beyond the meso-level. Experimental studies are extremely difficult at this size-scale in particular observation of the ITZ. Numerical simulation is an option that could give insight into the problem that cannot be obtained completely by means of experiments. Thus in this paper a numerical approach to the drying shrinkage problem is specified.

A lattice model for (semi-) coupled moisture flow and cracking of concrete due to drying shrinkage is presented. A Lattice Gas Automaton (Frisch et al. 1986) is coupled to an existing Lattice Fracture Model, developed at TU Delft. Both models originate from statistical physics and successfully simulate the behaviour of non-homogeneous porous media. The complex process of flow in porous media includes surface tension, capillary condensation, gas phase flow, surface and liquid flow (see Quenard & Sallee 1992 for an overview) which are excluded from the LGA at this stage. In the Lattice Fracture Model, a simple strength-based failure criterion is used (Schlangen & Van Mier 1992). The Lattice Fracture Model normally includes the meso- or microstructure of concrete. At this moment, the microstructure of cement in LGA has been included statistically.

2 Numerical Modeling of Moisture Flow

2.1 Lattice Gas Automaton

In order to describe motion of an incompressible Newtonian fluid, the Navier-Stokes, continuity equation and thermodynamic equation of state are used. Solution of the partial differential Navier-Stokes equation gives extreme mathematical difficulties due to the non-linearity. The exact solution can be found for a very few cases: parallel flow through a channel, the Hagen-Poiseulle flow through a pipe and a few more. Many other problems could be solved only by the application of an approximate solution of the partial differential equation such as conversion and integration with finite difference method, usually seen in finite element programs. Sadouki & Van Mier (1996) used this approach for simulating flow in porous media.

Other approximate solutions are the cellular automata (Wolfram 1986). A cellular automaton consists of a population of fluid particles in cells, which propagate and collide obeying a set of rules. A variant of cellular automata is the Lattice Gas Automaton (LGA) developed by Frisch, Hasslacher and Pomeau (Frisch et al. 1986). Instead of solving Navier-Stokes equations numerically, Lattice Gas Automata were introduced as a model of the Navier-Stokes equations.

The Lattice Gas Automaton (FHP model) is shown schematically in Figure 1a. A triangular lattice is populated with randomly distributed fluid particles, which propagate and collide according to the prescribed collision rules given in a lookup table (Frisch et al. 1987). When propagating on the regular triangular lattice (Noullez 1990), collision among particles can not be avoided (compared to the irregular lattice, Wolfram 1984). In the present study, the FHP model with six moving particles and one at rest is used (Frisch et al. 1987). The particles have unit mass and velocity.

The problem of moisture flow simulation with Lattice Gas Automaton is considered first in 2-D (Fig. 1b) in order to develop principles that later on could be included in 3-D calculations. The real pore structure of materials like cement is a complicated 3-dimensional network, which should be considered in 3-D simulations. The fluid flow in a porous medium is already a highly complex problem even when considered in two-dimensions. LGA is a simple computational model in 2-D, whereas in 3-D the calculations become too complicated (see Frisch et al. 1987).

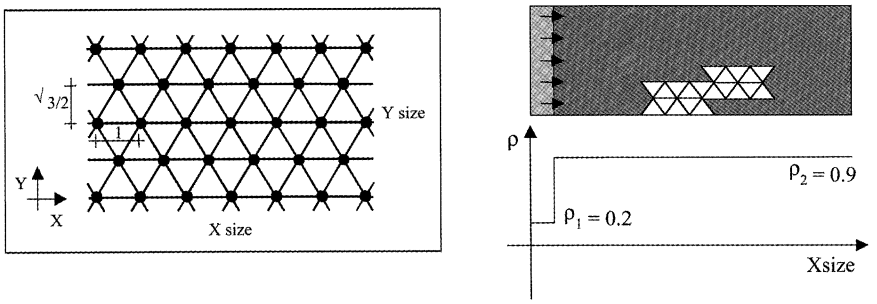

(a) (b)

Figure 1. (a) Lattice Gas Automaton and (b) Schematic presentation of LGA model with the distribution of densities in the initial stage.

Hence, for most problems in 3-D, LGA has to be replaced by the Lattice Boltzmann Method (Rothman & Zaleski 1997). This method solves the calculation problems and the noisy results of LGA, as well as some other lattice gas drawbacks. Nevertheless, in view of the physical nature of moisture flow, preferences are given to the LGA at this stage of the research.

2.2 Flow in homogeneous and heterogeneous media

The lattice is initially populated with the fluid particles such that higher density i.e. moisture content (density of the particles, $\rho = \sum_i N_i$, see Frisch 1986) is created. In order to invoke particles to propagate and collide and to model simultaneously one-sided (left side) drying, it is necessary to simulate changes of the moisture content. Consequently particles are inserted at the left edge of the lattice with zero velocity in x- and y-direction (u = v = 0) creating a lower density zone. In the present analyses (Fig. 1b), the initial moisture content in the sample was $\rho = 0.9$, while the introduced new moisture level was $\rho = 0.2$. Similar models can be found in the literature. The researchers were typically discussing saturation with Lattice Gas Automaton in 2-D, where the 'feeding' of lattice with a higher moisture content was applied, e.g. Küntz et al. 2001.

Computational LGA time increases substantially with the increase of the lattice node (site) numbers. In order to avoid this problem and to be able to couple LGA with the existing fracture model, the size of LGA is taken as $1000 \times 100\sqrt{3}/2$ in x and y direction respectively. Space averaging is usually carried out in order to diminish the noise in LGA results. In this process, the average was taken over blocks Xsize x Ysize = 8 x 8 nodes which gave satisfying results. In the very first analysis a homogeneous lattice was considered, whereas in the second analysis a large obstacle was placed in

the center. Although treated as homogeneous, the first sample was also populated with a small percentage (3%) of randomly distributed solid particles. In Boolean algebra, this is expressed as the addition of the extra bit marked 1, to represent the existence of a material point (Frisch et al. 1987, d'Humières & Lallemand 1987, Noullez 1990).

Periodic boundary conditions were applied in the vertical direction by default. The sample was closed at the left side with a boundary wall in order to prevent re-entrance of the particles. Different boundary conditions can be selected between solid and fluid particles: for example, with the presence of wall or with material particles in the microstructure. Two types of boundary conditions were applied here: specular reflection (free-slip boundary condition) or bounce-back reflection (no-slip boundary condition). Both types can be used for the microstructure points. Only the bounce-back reflection was applied on the left wall.

In the first example (homogenous sample in Jankovic et al. 2001), 90000 steps were carried out to dry out the sample. The results from every 5000 steps were recorded. In the second analysis, flow in a heterogeneous sample was simulated with a big obstacle embedded in the cement matrix. The number of steps required for the drying of the sample was much lower (15000), which could be explained by the presence of less fluid particles in the sample since a relatively large space was occupied by the large 'solid' obstacle. The height of the obstacle was $^1/_2$ of the sample height. A more detailed description can be found in Jankovic et al. 2001.

In the present study the 12-collision rule was applied from the collision lookup table. The type of the collision rule is very important since it affects the transport properties of the lattice gas. If the collision rate is low (minimum 5 collision rules must be present, d'Humières & Lallemand 1987) then both viscosity and diffusion (Noullez 1990) are high (Rothman & Zaleski 1997). In order to improve the qualitative behaviour of the lattice gas, the viscosity has to be lowered i.e. collision rate higher with the addition of particle at rest (Frisch et al. 1987).

2.3 Drying shrinkage curves

The drying process can be followed from the drying profiles where moisture distributions are shown in the homogeneous sample (Fig. 2) for both boundary conditions r = 1 and r = 0 (Jankovic et al. 2001). The calculation was made along the Xsize of the lattice taking into account the average density value of every point across the height of the sample.

The simulation with bounce-back reflection r = 0, Figure 2b, showed a steeper moisture gradient after the first 5000 steps compared to the drying profiles with specular reflection (r = 1). Later on, the moisture loss was substantially slower. The speed of drying is influenced by averaging over different size of blocks (4 x 4 or 8 x 8), higher or lower rate of collision, the presence or absence of the boundaries at the top and bottom and by the choice of either specular or bounce-back reflection. A higher degree of the averaging leads to quicker particle loss. When the collision rate is increased, the viscosity is decreased and the sample dries out much quicker. Periodic boundaries increase the loss of particles and subsequently accelerate the drying. Boundary conditions define the velocity of fluid. With the bounce-back reflection, the sign of the particle velocity is opposite to the incoming velocity, which slows down the drying process.

3 Lattice Fracture Model (LFM)

For the fracture simulations an elastic-purely brittle Lattice Fracture Model has been used, Schlangen & Van Mier (1992). In the LFM the continuum is discretized as a regular or random network of beam elements, where load is applied in the nodes only. The advantage of such lattice models is the simple fracture law that can be used, which is especially important when microstructure is implemented. An elastic-purely brittle law was used to break the beams. Since microstructure was included directly in the mesh, non-linearity from material structure should appear directly. In contrast, in continuum-based fracture models, more complicated softening fracture laws must be used.

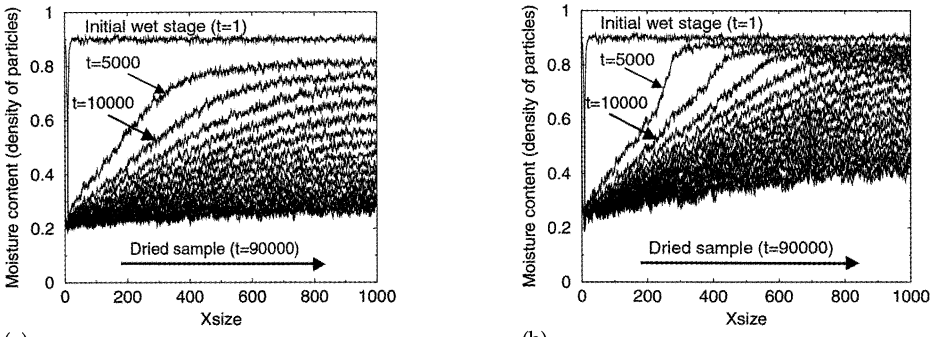

Figure 2. Density (moisture content) profiles due to drying at various time-steps for different boundary conditions (a) specular reflection (r = 1) and (b) bounce-back reflection (r = 0).

The mesostructure is included in the fracture analysis projecting the three-phase material (aggregate, interface zone or cement matrix) on top of the lattice. Two groups of parameters are necessary in the model. The first group of parameters is related to the stiffness of the mesh such as the cross sectional area of the lattice beam and the Young's modulus of the material. The second group concerns the fracture law itself: the value of the tensile strength f_t depends on the location of a beam in a specific material (aggregate, interface zone or cement matrix), Van Mier et al. (1995).

4 Coupling of Lattice Gas Automaton and Lattice Fracture Model

The geometry of the meshes used in LGA and LFM looks the same: in both cases a regular triangular mesh with hexagonal symmetry is used. The similarities in geometry allow for easy superposition of the two models. The coupling between LGA and LFM was done via an expression for the shrinkage strain and stress (Eqs 1-2) and nodal force in the lattice beams (Eq. 3) as follows:

$$\varepsilon_{sh} = \alpha_{sh} \Delta h \tag{1}$$

$$\sigma_{sh} = \varepsilon_{sh} E \tag{2}$$

$$F = \sigma_{sh} A \tag{3}$$

where ε_{sh} is a shrinkage strain, α_{sh} is a shrinkage coefficient , Δh is a moisture gradient, σ_{sh} is a shrinkage stress (MPa), F is a nodal axial force (N), E is Young's modulus (MPa) and A is a lattice beam cross section (mm^2). The moisture gradient Δh was calculated from the LGA between two central nodes of neighbouring, averaging blocks for a certain number of steps (e.g. every 1000 or 5000 step). The resultant 'pre-stress' moisture load (Eq. 3) was applied as axial forces to the respective beam elements in order to give the crack patterns. The applied nodal forces can be either tensile or compressive since the moisture distributions are non-uniform. Consequently shrinkage strains and stresses are distributed non-uniformly as well. A more detailed description can be found in Jankovic et al. 2001.

5 Resulting drying-crack patterns

Since we are interested in the development of crack patterns, the major concern is to find the LGA time-steps, sufficiently critical to induce cracking. According to the drying curves of the homogeneous sample (Fig. 2), the very first step has the highest moisture gradient (Eq. 1) in the case of both boundary conditions. The gradient was also high for smaller steps (every 1000^{th} step up to maximum of 5000 steps, Fig. 3a) specifically for the bounce-back boundary condition being crucial for the shrinkage deformation and crack development. Subsequently, an analysis was made where the calculated 'pre-stress' forces were saved every 1000^{th} LGA step up to a total of 5000 steps.
For the sample with the central obstacle, the LGA output was also recorded for every 1000^{th} step (Fig. 3b). The sequence of every 1000^{th} steps was chosen arbitrarily in both cases and used as one input step in LFM in order to calculate a new crack pattern. In this case drying curves look different. The steep moisture gradient develops in the initial stage but also around the aggregate in the subsequent stages. In general, the shape of the drying curves is irregular due to the boundary conditions and the small height of lattice (Ysize) compared to the big size of the obstacle (see Jankovic et al. 2001). The drying curve diagram (Fig. 3b) may also imply that drying around the aggregate is independent from the surface drying.
Various results from the lattice coupling are shown. Deformations and axial stresses (σ_{xx}) in the homogeneous sample are presented in Figure 4. They were calculated with the DIANA finite element code where the Lattice Fracture Model was implemented. Cracks appear from the zone where drying occurs first (where the moisture gradient is the highest) in the form of the missing beams. Drying deformations are shown by the change in the gray levels in the figure.

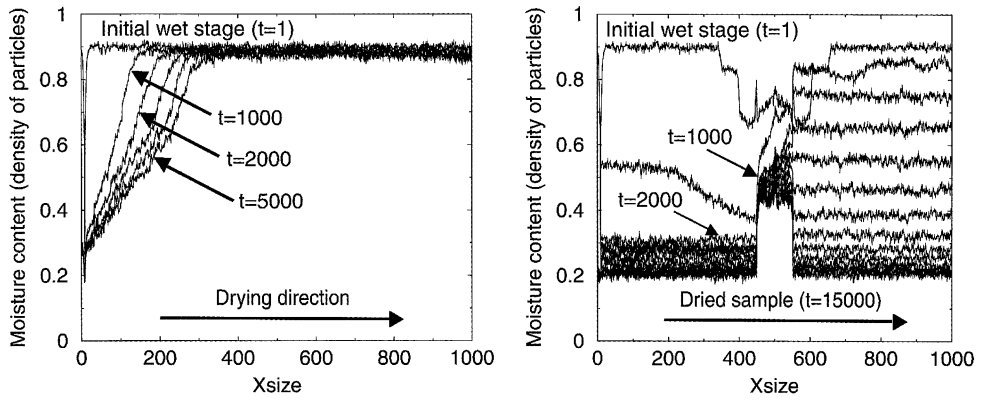

(a) (b)

Figure 3. (a) Density (moisture content) profiles due to drying with the application of bounce-back reflection (r = 0), every 1000th step recorded in homogenous sample (up to max of 5000 steps), (b) complete drying in 15000 steps for the sample with large obstacle.

Concentration of the highest tensile and compressive stress occur in the region where drying begins. The crack pattern is very discontinuous, which seems to be caused by local variations in the moisture distribution, by the randomly distributed solid particles but also by the support locations. On the other hand discontinuity in the crack patterns should occur to some extent, as confirmed by the observations of Xi & Jennings 1992.

In the analysis with the large aggregate particle (Fig. 5), cracks appeared around the obstacle in the interface zone. These results must be taken with some precaution since the number of steps was insufficient for a prediction of further crack propagation. Second, the aggregate (obstacle) was located far from the surface. The height of the specimen was very narrow compared to the height of the obstacle which was a limitation for fluid flow around it. Moreover there are doubts if the flow at the surface of the aggregate is modelled in the right way.

This model should be treated as a special case since it did not have any experimental approvals yet.

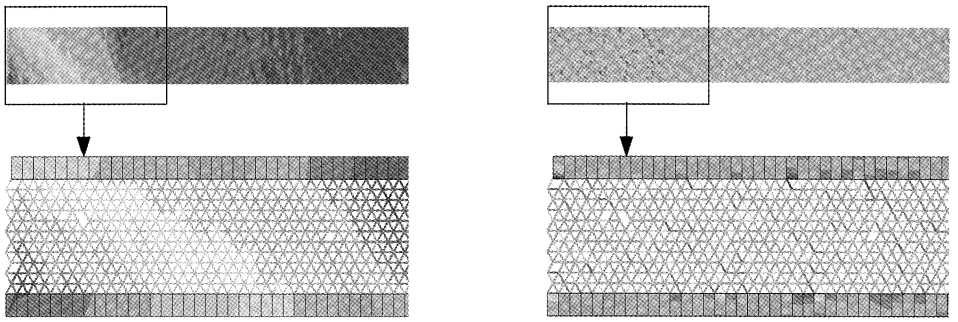

(a) (b)

Figure 4. (a) Deformations d_x and (b) σ_{xx} stresses in a homogeneous sample after 5000 LGA steps (r = 0).

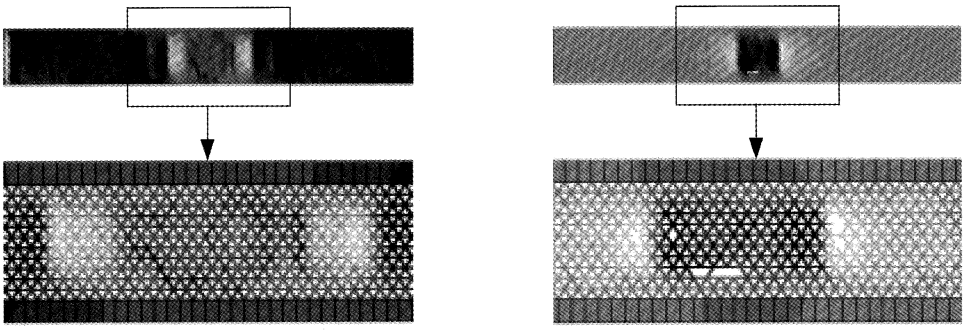

(a) (b)

Figure 5. Deformations and cracks in LFM, (a) after 1000th step in LGA, r = 0, (b) after 15000 steps in LGA, r = 0.

Experiments on drying shrinkage usually had more than one aggregate embedded in the cement paste matrix located at various distances from the surface or one aggregate embedment dried under various conditions. In the experiments described by Van Mier & Bisschop (2001), aggregates of different sizes were randomly distributed in the cement paste. The size of the aggregates as well as their location in the cement paste (close or distant from the surface) played important role for the cracking mechanisms. In the case of larger aggregates close to the surface, two restraining mechanisms, self-restraining and aggregate restraining were interacting. Cracks radiated out from the surface aggregates and developed vertically into the specimen. There is still no experimental evidence to prove which of the mechanisms (self-restraining or aggregate restraining) would prevail to cause first crack pattern in concrete due to drying shrinkage. Experiments with one aggregate placed far away from the surface could resolve this question.

6 Discussion

It is known from the mechanics of the materials that an increase of the load will increase deformations and stresses in the sample. In the case of drying shrinkage process, there is no other load but moisture flow, which causes differential deformations (Eq. 1) due to a moisture gradient.
According to the applied strength criterion in the Lattice Fracture Model, cracks will occur when the tensile (shrinkage) stress (Eq. 2) exceeds the tensile strength of the material. Thus when the results from LGA are combined with LFM, the increase in number of 'drying' (load) steps results in the increase of cracks (every 1000th or 5000th step in LGA is used as one load step in LFM and consequently one beam is broken). This could suggest that as long as the sample is drying, the shrinkage deformations and stresses would increase and possibly produce a crack.
The expression (1) states that the shrinkage deformations linearly increase with the moisture gradient (a constant value for the shrinkage coefficient was assumed from the literature, Martinola & Wittmann 1995). From the drying curves (Fig. 2), it is apparent that when the number of LGA steps increases, the moisture gradient decreases and finally a dried sample with equally distributed low moisture content is obtained. This is probably the time-step when shrinkage cracking would end due to the low moisture content since no other source of deformation is present.

If the Eq. 1 is linear then the network of cracks could develop very quickly in very early stages of drying due to the high moisture gradient in the first steps. These cracks could expand only on the surface following the strength criterion. Further crack growth might be influenced by the fracture energy criterion. In that case there should be enough energy for cracks to develop beyond the surface since the induction of the cracking already exists. The other explanation could be the non-linear relation (shrinkage coefficient α_{sh}) between the shrinkage deformations and the moisture gradient (Eq. 1). The solution key to these assumptions lies in the experiments, which should give better insight into the nature of drying shrinkage.

This discussion applies to the homogeneous material where self-restraining due to the moisture gradient is one of the leading mechanisms. In the case of heterogeneous materials (i.e. concrete), when stiff aggregates are present, the moisture flows around the aggregate. This may cause differential stresses and microcracking as the mismatch in Young's modulus of the aggregate and matrix elements so that stress concentrations appear in the interfacial transition zone. Since ITZ is extremely porous, the highest shrinkage could occur there.

The cracking in the LFM is solved in such way that always one beam is broken and removed with one LGA step. The removal of one beam refers to a simple crack occurrence. In the coupling with LGA, it is hard to tell how many beams should be broken at a given time-step. This would naturally influence the crack patterns. Certain LGA steps may possibly develop more cracks compared to the others. Additional changes in the fracture criterion in the Lattice Fracture Model might solve this problem. The crack patterns, which the moisture load from every LGA step induces, should develop as long as the adjusted fracture criterion is not fulfilled. It must be emphasized again that time-steps in LGA are not yet defined in terms of 'real' time (hours, etc.). We also do not know to which length-scale to apply our numerical model to make an adequate comparison (i.e. length of cracks or others) with any experimental results.

The two lattice models are still 'semi-coupled'. This means that when the crack occurs in LFM, no changes were made to the following LGA steps. In reality, the complex cement microstructure contains both empty pores and pores filled with water. In LGA it is assumed that the whole sample is completely saturated and that initial pre-stress is present at every node in the Lattice Fracture Model. Since no complex microstructure has been implemented in the model to define pore spaces, the complete coupling is skipped at the present moment. These dilemmas need yet to be adequately tackled.

7 Conclusions

First steps have been taken in the development of a numerical model to simulate drying shrinkage cracking in concrete and more particular in the interfacial transition zone between cement and aggregate. Due to their geometrical similarities two lattice models, namely Lattice Gas Automata and Lattice Fracture Model, were 'semi-coupled' in order to simulate crack pattern caused by drying shrinkage.

The Lattice Gas Automaton was used for the moisture flow simulations of drying in homogeneous and heterogeneous samples. These samples represent cement paste and cement paste with a large obstacle in the middle. At this moment, the model does not represent the microstructure of cement paste. As observed in the experiments (e.g. NMR presented in Bisschop et al. 2001), drying of cement paste causes shrinkage deformations, which produces high tensile stress-concentrations in the cement paste structure and subsequently shrinkage microcracks. Due to that, Lattice Gas Automaton was combined to the Lattice Fracture Model (embedded in DIANA finite element code) which resulted in the 'drying' shrinkage-crack pattern.

The main problem is scaling of LGA steps to the time-steps (hours or days) in real drying experiments. Fine-tuning of the model is essential, as is the determination of the so-called drying shrinkage coefficient α_{sh} at a sufficiently small scale. The α_{sh} coefficient is assumed to be a property of cement and it will vary for different cement types under different drying conditions. Hence future developments will focus on the inclusion of a realistic cement microstructure and measurement of salient model parameters in laboratory experiments.

Acknowledgement

This research is supported by a grant from the Priority Programme Materials Research (PPM) and the Dutch Technology Foundation STW, which is gratefully acknowledged.

References

Bisschop, J., Pel, L. & Van Mier, J.G.M. "Effect of Aggregate Size and Paste Volume on Drying Shrinkage Microcracking in Cement-based Composites", in *Creep, Shrinkage and Durability Mechanics of Concrete and Other Quasi-Brittle Materials, Proceedings CONCREEP-6*, (Ulm, F.-J., Bazant, Z.P. and Wittmann, F.H. eds.), Elsevier Science, Amsterdam, 2001, pp. 75-80.

d'Humières, D. & Lallemand, P. "Numerical Simulation of Hydrodynamics with Lattice Gas Automata in Two Dimensions", *Complex Systems* 1, 1987, pp. 599-632.

Frisch, U., Hasslacher, B. & Pomeau, Y. "Lattice-gas Automata for the Navier-Stokes Equation", *Physical Review Letters* 14 (56), 1986, pp. 1505-1508.

Frisch, U., d'Humières, D., Hasslacher, B., Lallemand, P., Pomeau, Y. & Rivet, J-P. "Lattice Gas Hydrodynamics in Two and Three Dimensions", *Complex Systems* 1, 1987, pp. 648-707.

Jankovic, D., Küntz, M. & Van Mier, J.G.M. "Numerical Analysis of Moisture Flow and Concrete Cracking by means of Lattice Type Models" in *Proceedings FraMCoS – 4*, (R.de Borst, J. Mazars, G.Pijaudier and J.G.M. van Mier, eds.), Balkema, Rotterdam, 2001, pp. 231-238.

Küntz, M., Van Mier, J.G.M. & Lavallée, P. "A Lattice Gas Automaton Simulation of the Non-linear

Diffusion Equation: A Model for Moisture Flow in Unsaturated Porous Media", *Transport in Porous Media 43*, 2001, pp. 289-307.

Martinola, G. & Wittmann, F.H. "Application of Fracture Mechanics to Optimize Repair Mortar Systems", *Fracture Mechanics of Concrete Structures, Proceedings FRAMCOS-2*, ed. Wittmann, F.H., 1995.

Noullez, A. "Automates de Gaz sur Reseaux: Aspects théoriques et simulations", PhD thesis, Université Libre de Bruxelles 1990.

Quenard, D. & Sallee, H. "Water Vapour Adsorption and Transfer in Cement based Materials: a Network Simulation", *Materials & Structures (RILEM)* 25, 1992, pp. 515.

Rothman, D.H. & Zaleski, S. "Lattice-Gas Cellular Automata: Simple Models of Complex Hydrodynamics", *Cambridge University Press* 1997.

Sadouki, H. & Van Mier, J.G.M. "Meso-level Analysis of Moisture Flow in Cement Composites using a Lattice-Type Approach", *Materials & Structures (RILEM)*, 30, 1997, pp. 579-587.

Schlangen, E. & Van Mier, J.G.M. "Experimental and Numerical Analysis of the Micro-mechanisms of Fracture of Cement-Based Composites", *Journal of Cement and Concrete Composites* 14, 2, 1992, pp. 105-118.

Van Mier, J.G.M., Schlangen, E. & Vervuurt, A. "Lattice Type Fracture Models for Concrete", in *Continuum Models for Materials with Microstructure*, ed. H.B. Mühlhuis, John Wiley & Sons Ltd. 1995, pp. 341-377.

Van Mier, J.G.M. & Bisschop, J. "Microscopy study of Shrinkage Microcrack Mechanisms as a Basis for Durability Mechanisms of Concrete" *8th Euroseminar on 'Microscopy Applied to Building Materials'*, Athens, 2001(key-note paper)

Wolfram, S. "Universality and Complexity in Cellular Automata", *Physica 10D*, 1984, pp. 1-23.

Wolfram, S. "Cellular Automaton Fluids 1: Basic Theory", *Journal of Statistical Physics 45*, 1986, pp. 471-526.

Xi, Y. & Jennings, H.M. "Relationships between Microstructure and Creep and Shrinkage of Cement Paste", *Material Science of Concrete* III, 1992, American Ceramic Society, pp. 37-69.